Characterization of bubble column photobioreactors for shear-sensitive microalgae culture

Lorenzo López-Rosales[1], Asterio Sánchez-Mirón[1,2*], Antonio Contreras-Gómez[1], Francisco García-Camacho[1,2], Francine Battaglia[3], Lei Zhao[4], Emilio Molina-Grima[1,2]

[1] Dept. of Chemical Engineering, University of Almería, 04120 Almería, Spain

[2]Research Center in Agrifood Biotechnology, University of Almería, 04120 Almería, Spain

[3]Department of Mechanical and Aerospace Engineering, University at Buffalo, New York, 14260, U.S.A.

[4]Department of Mechanical Engineering, Virginia Tech, Blacksburg, Virginia, 24061, U.S.A.

* Author for correspondence

Dept. of Chemical Engineering, University of Almería,

04120 Almería, Spain

e-mail: asmiron@ual.es

Graphical Abstract (for review)

Accepted manuscript. https://doi.org/10.1016/j.biortech.2018.12.009

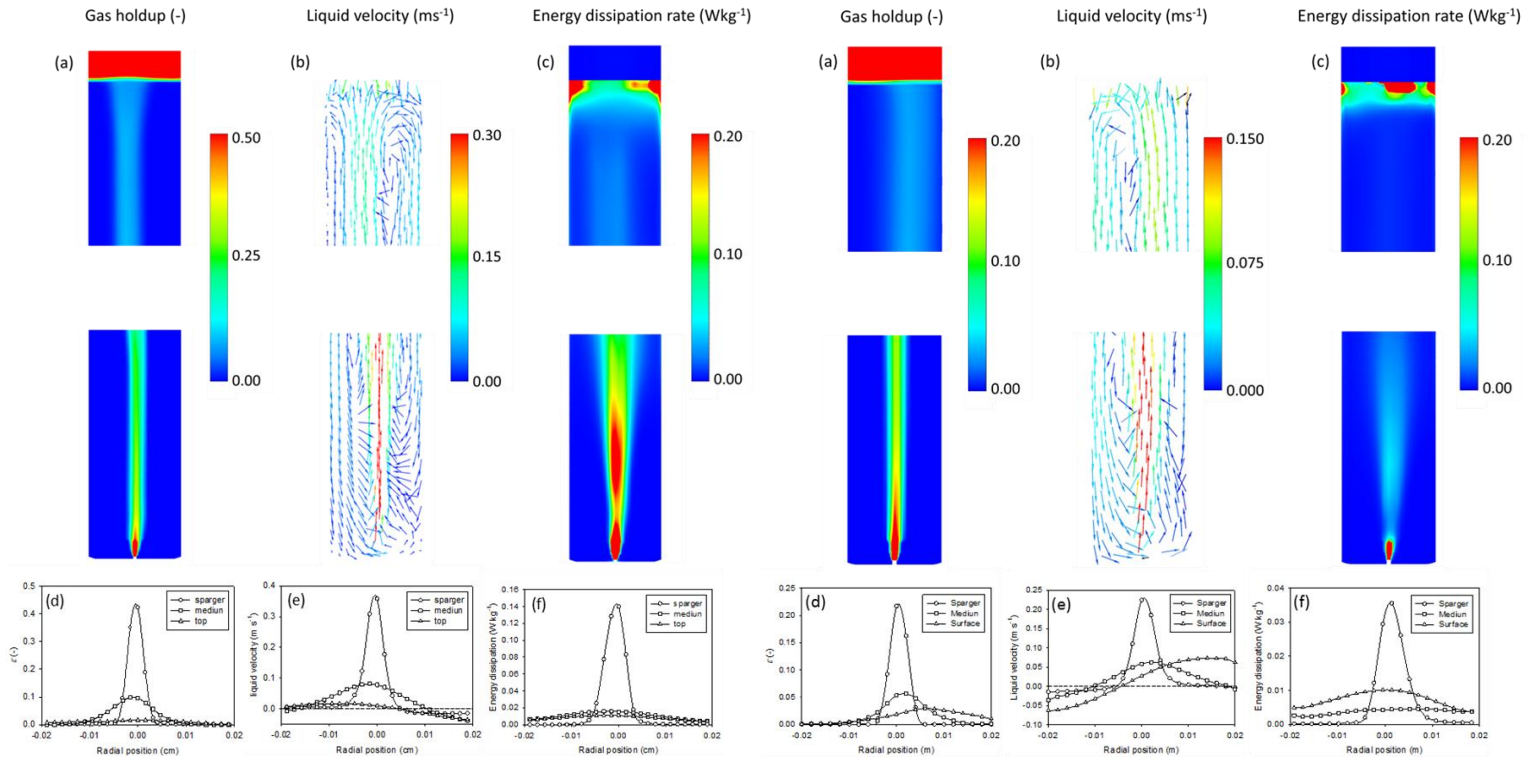

Abstract

The shear-sensitive marine algal dinoflagellate *Karlodinium veneficum* was grown in a cylindrical bubble column photobioreactor with an internal diameter of 0.044 m. Initial liquid height varied from 0.5 to 1.75 m, superficial gas velocities from 0.0014 to 0.0057 ms^{-1}, and nozzle diameter from 1 to 2.5 mm. Computational fluid dynamics was used to characterize the flow hydrodynamics and energy dissipation rates. Experimental gas holdup and volumetric mass transfer coefficient strongly depended on the liquid height and correlated well with the Froude number. Energy dissipation near the head space (ED_{top}) was one order of magnitude higher than the average energy dissipation in the whole reactor (ED_{whole}), and the value in the sparger zone (ED_{spar}) was one order of magnitude higher than ED_{top}. Cultures of *K. veneficum* were limited by CO_2 transfer at low ED_{whole} and severely stressed above a critical value of ED_{whole}.

Keywords: *Karlodinium veneficum*, bubble column, CFD, cell damage, energy dissipation rate

1. Introduction

Bubble columns are widely used as multiphase reactors because of their simple construction and operation. They are used in chemical, metallurgical and biochemical processes (Ferreira et al., 2013), providing a competitive alternative in two- and three-phase processes with mass and heat transfer limitations, where efficient interphase contacting is needed (Nedeltchev et al., 2014). A bubble column is also a popular configuration for closed photobioreactors that has received considerable attention over the last decade (Pegallapati and Nirmalakhandan, 2012, Bitog et al., 2014, Manjrekar et al., 2017, López-Rosales et al., 2017). The bubble column provides a number of advantages over other photobioreactor configurations such as simplicity in design and construction with no moving parts, ease of operation, small floor space requirements, excellent heat transfer characteristics and temperature control, and suitable interphase mass transfer at low energy input. Nonetheless, due to a lack of knowledge on the complex bubble-liquid hydrodynamics and its influence on transport process, cell growth, and scale up, bubble column photobioreactors are still not well understood. Hydrodynamics in bubble columns are determined by gas sparging at the bottom section. Gas injection is essential for microalgae culture processes, driving the flow and mixing, and indeed mass transfer and light penetration and distribution. However, bubble formation at the sparger, its upward movement, and rupture at the culture surface can produce significant shear forces in small regions that can potentially induce cell damage. Bubble-associated cell damage has been studied extensively in animal cells. Since the early works, before 1990, bubble rupture at the culture surface is believed to be responsible for most of the cell deaths (Hu et al., 2011, Liu et al., 2014; Zhu et al., 2008). However, studies with microalgae are more limited. In an early study, Suzuki et

al. (1995) found a linear relationship between specific rate of cell death of *Dunaliella tertiolecta* and the inverse of culture height. This relationship implies that cell damage is solely due to bubble rupture. Contreras et al. (1998) found a relationship between growth rate of *Phaeodactylum tricornutum* and the presence of bubbles in an airlift photobioreactor, whereby decreasing growth rate was related to increasing shear rate. García-Camacho et al. (2000) observed a positive linear relationship between death rate and culture height for *Porphyridium cruentum*. The author suggested that cells attached to rising bubbles were carried to the culture surface and damaged during bubble rupture. The critical role of cell-bubble attachment in cell death due to bubble rupture was also demonstrated by Meier et al. (1999). Barbosa et al. (2003) found the most significant microalga cell damage in the region near the sparger due to bubble formation, and subsequently determined a critical gas entrance velocity that induced good mixing without harming cells. Recently, López-Rosales et al. (2017) investigated the growth of the shear-sensitive dinoflagellate microalgae *Karlodinium veneficum* in a bubble column. According with their studies, bubble break-up at the gas-liquid interphase was much more detrimental for cells than bubble formation at the sparger.

Since complex hydrodynamics of sparged bioreactors prevent the use of simple correlations relating cell response to a specific condition in a bioreactor (Hu, Berdugo, Chalmer, 2011, López-Rosales et al., 2017), in parallel with the aforementioned experimental studies, attempts of theoretical or computational studies have been reported to obtain insights into the sparging-associated cell damage. Traditionally, different hydrodynamic parameters have been used to correlate cell damage in photobioreactors, including shear rate or shear stress (Silva et al., 1987; Gudin and Chaumont, 1991; Contreras et al., 1998), micro-eddy length scale using Kolmogorov's theory (Contreras et al., 1998) and energy dissipation rates (*ED*) (Contreras et al., 1998)

are the most widely used. Nonetheless, although different hypotheses have been proposed, little is known about sparging-associated mechanisms of microalgae cell damage at a fundamental level (López-Rosales et al., 2015, 2017).

This paper utilizes computational fluid dynamics (CFD)-assisted characterization of a bubble column photobioreactor to interpret the shear-sensitivity responses of the marine microalga *K. veneficum*. Different parameters influencing microalga growth (gas holdup, liquid velocity, energy dissipation and mass transfer) were studied and correlated with dimensionless Froude number. *ED* in different zones of the PBR were found to be dependent on each other. *ED* has been previously used to characterize cell damage in different reactors and laboratory equipment (Contreras et al., 1998; Mollet et al., 2004). However, in this paper, we have integrated the energy dissipation rate field in the photobioreactor into an existing growth model that has been successfully extrapolated to other scaled-up sparged photobioreactors. To the authors' knowledge, this methodology is used here for the first time in dinoflagellate cultures, and will be of great help in the scaling-up process of aerated cultures of shear-sensitive microorganisms.

2. Material and methods

2.1. Database

The environment to which the cells are subjected inside a bubble column photobioreactor is governed mainly by the system design (including culture height, internal column diameter, and sparger geometry) and working parameters (gas flow rate). These variables govern gas velocity at the sparger, gas holdup, bubble diameter, interfacial area and, ultimately, mass transfer, but these variables are also responsible for different mechanisms of cell damage. In this work a database of a genetic algorithm-

based search for optimal culture conditions (gas flow rate, *Q*, initial culture height, *H*, and nozzle sparger diameter, d_0) for *K. veneficum* in a bubble column photobioreactor was used (López-Rosales et al., 2015). This database comprises 25 experiments with different combinations of *Q*, *H*, and d_0 described elsewhere (López-Rosales et al., 2015) of which 8 representative combinations have been simulated.

Briefly, inocula were grown in shake flasks at 18±1 °C under continuous irradiance at the surface of the culture flasks (300 $\mu Em^{-2}s^{-1}$). L1 medium (Guillard and Hargraves, 1993) prepared using filter-sterilized (0.22 µm Millipore filter; Millipore Corporation, Billerica, MA, USA) Mediterranean Sea water was used to grow inocula and all subsequent cultures. Experiments were carried out in vertical clear plastic (polymethyl methacrylate) cylindrical bubble columns (internal diameter D = 0.044 m; height of 2 m). Initial culture heights, *H*, ranged between 0.5-1.75 m (which corresponds to H/D aspect ratios from roughly 11 to 40). Cultures were agitated by filtered air sparging from a compressor injected through a single-nozzle sparger with nozzle diameters ranging from 1 to 2.5 mm. The superficial air velocity during the culture ranged between 0.0014 and 0.0057 ms^{-1}. The experiments were performed in duplicate at the same time. To prevent interferences of nutritional limitations, the cultures were finished after 5 days (López-Rosales et al., 2015).

The database (López-Rosales et al., 2015) was supplemented with a database of parameters (bubble diameter, d_b, gas holdup, ε, and volumetric gas-liquid mass-transfer coefficient, k_La) originally carried out to study of how hydrodynamic stress and mass transfer influence on cell growth of *K. veneficum* (López-Rosales et al., 2017). Overall gas holdup was obtained by total volume displacement. The overall volumetric mass-transfer coefficient, k_La, for O_2 was measured by the well-established gassing-in method (Sánchez-Mirón et al., 2000) using a fast-response dissolved-oxygen electrode. K_La for

CO_2 was calculated according to penetration theory, multiplying k_La for O_2 by the factor 0.91 (Molina-Grima et al., 1993). The experiments were performed in duplicate.

2.2. Computational fluid dynamics (CFD)

Computational fluid dynamics was used to simulate and characterize the flow field, and map the local *ED* in various zones of the photobioreactors. Previous work by Zhao et al. (2016a,b) was used to further justify the use of the computational models presented here.

The time-dependent simulations were performed using ANSYS Fluent® v16.2 (www.ansys.com) software. As we were interested in the time average value of the variables, the realizable k-ε turbulence model was used. An implicitly formulated Eulerian two-phase model was used to describe the gas-liquid interactions. The liquid velocity at the solid walls was taken to be zero (i.e. non-slip condition). In all simulations the continuous phase was seawater (density = 1,023 kg m^{-3}, viscosity = 1.28×10^{-3} Pa s) and the dispersed phase was air (density = 1.225 kg m^{-3}, viscosity = 1.789×10^{-5} Pa s). Viscosity of the cell suspension at the inoculation time was the same as sea-water. Viscosity was checked along the culture time and measurable variations in the culture viscosity with the culture time were not observed. Therefore, the sea-water properties were used in all the simulations. Only the drag force was considered between phases and was estimated using the Grace model. A surface tension of 71.8×10^{-3} N m^{-1} was used.

The outlets of the bioreactors were modeled as pressure outlets (P = 1 atm) with an air volume fraction of 1. The air inlets were modeled as mass inlets, with an air volume fraction of 1. Simulations used a pressure-based model under transient conditions.

Gravity was included in the model in the negative *z*-direction. The pressure reference was fixed at the outlet. The other models employed were SIMPLE for the pressure-velocity coupling; Least Square Cell Based for Gradient (LSCBG) scheme for spatial discretization; QUICK for momentum; modified HRIC for volume fraction; and second-order upwind discretization for turbulent kinetic energy and dissipation rate.

In general, the time step size was not fixed higher than 1×10^{-3} s with a maximum of 25 iterations per time step to ensure residuals dropped three orders of magnitude. Once the flow and the air mass flow rate stabilized, the data were time averaged for 30 s with a data sampling interval of 0.01 s.

The mesh was generated with cut cell assembly method to obtain perfectly hexahedral cells aligned with the flow to minimize errors associated with numerical diffusion. The optimal mesh size was obtained from a mesh sensitivity analysis based on the radial velocity profiles. The cell size was fixed at 0.5 mm in the sparger zone and the maximum face size of the optimum mesh was 2 mm.

Energy dissipation rates were calculated using the last 30 s of the simulations as volume weighted averages. The average values were obtained in Ansys-Post from data exported every 0.5 seconds, as Fluent does not natively time-average this variable. For the calculation in the sparger (ED_{spar}) and in the top gas-liquid interphase (ED_{top}), we selected the dispersion volume with a value a 30% lower than the maximum in each of the zones.

3. Results and discussion

The development of efficient CO_2 supply and oxygen removal systems is one of the most challenging topics in algal processes, particularly in closed photobioreactors.

Despite the efforts made over the years (Ferreira et al., 1998, Carvalho et al., 2006), air or CO_2-enriched air sparging remains the most popular and convenient method of supplying CO_2 and removing oxygen from microalgae culture in large-scale photobioreactors. Therefore, *Q* is a crucial parameter to determine the environment for cell growth. Inlet gas should provide an efficient mixing to maintain microalgae in suspension, avoiding gradients of nutrient concentration and temperature and providing a sufficient light distribution with a homogeneous average exposure to light. However, hydrodynamic forces associated with gas sparging may lead to impaired cell growth or even cell damage or cell death of sensitive microalgae (López-Rosales et al., 2015).

In this work, the hydrodynamic of a bubble column photobioreactor was studied and simulated using CFD at different operating conditions described in the previous section. The values for superficial gas velocity, U_g, (< 0.0057 ms^{-1}) produced bubbles that rise individually, without interacting. This is in line with a previous study (López-Rosales et al., 2017) in which it was shown that the range of superficial gas velocities used in the study presented herein is well within the homogeneous bubbly flow regime and that the heterogeneous regime is not reached.

Fig. 1 shows gas holdup, liquid velocity and local energy dissipation rate averaged over 30 seconds in a longitudinal x-y plane and radial profiles at different locations of the longitudinal plane for the shortest column (H = 0.5 m, H/D = 11, U_g = 0.0028 m/s, d_0 = 1.5 mm). Fig. 2 shows the same parameters for the tallest column (H = 1.75 m, H/D = 40, U_g = 0.0014 m/s, d_0 = 2 mm). The gas leaving the nozzle in the sparger is the only source of energy in bubble columns photobioreactors used in this work. The momentum transfer between gas and liquid phases takes place in this region and the gas phase flow accelerates the liquid phase in a very low region, developing the well-established recirculating flow of the liquid phase, moving up with the bubbles in the gas plume and

moving down along the wall (Pfleger and Becker, 2001). The gas plume rises with fairly homogeneous velocity in all the combinations assayed. No evident gas plume distortion or transverse movement in any particular direction was detected in the shorter reactors, as presented in Fig. 1. Visual observations confirmed the homogeneous bubbly flow regime. The bubbles had almost identical sizes and shapes, spherical or hemispherical, and rose without collision, coalescence or division. This produces the characteristic symmetric parabolic radial profiles with a peak in the centre of the gas holdup profile (Fig. 1d). The maximum gas holdups are found just above the nozzle. Since the bubbles spread in the radial direction to some extent during their rise, this produces a flatter profile as bubbles move upward from the sparger. This spatial variation of gas holdup accompanies pressure variations, which drives liquid recirculation. In turn liquid recirculation determines mixing, and mass and heat transfer characteristics. Clearly, profiles of liquid axial velocity and energy dissipation are similar to gas holdup profiles, with maximum values found just above the nozzle and profiles become flatter when the distance from the sparger is increased (Fig. 1e,f). This is especially relevant for energy dissipation, since energy dissipation in the sparger region is one order of magnitude higher than the energy dissipation near the top of the photobioreactor, although the energy dissipated when one bubble bursts (Duchemin et al., 2002) will be much higher than the value in the sparger zone.

In taller reactors the behavior is similar, but the gas plume tends to rise near the wall at the top of the dispersion, and characteristic profiles of gas holdup, liquid velocity and energy dissipation were obtained (Fig. 2). Nonetheless, observed differences in the magnitude of gas holdup, liquid velocity and energy dissipation between the two systems are not due to different H, but to higher U_g and small d_0 in the shorter column. In a larger 80-L bubble column the dissipation rates had the same behavior but a

symmetrical liquid recirculation pattern and air hold-up where observed. In a flat panel photobioreactor plume distortions where observed at the bottom of the reactor due to liquid recirculation near the side walls (López-Rosales et al., 2018)

Prediction of gas holdup is of great importance in determining liquid circulation, mixing, and mass and heat transfer in bubble columns, and it is of critical importance in photobioreactors for microalgal culture. Therefore, many studies have been carried out during the past decades to elucidate the effect of Q, D, and gas and liquid properties (see Sasaki et al., 2016); and correlations have been proposed to predict both, radial gas holdup profiles (see Wu et al., 2001) and overall gas holdup (see Sasaki et al., 2016). Nonetheless, while it is well known that gas holdup decreases when initial liquid height increases, as far as we know the effect of liquid height has not been taken into account in correlations (see Sasaki et al., 2016).

Experimental overall gas holdup is plotted against superficial gas velocity, U_g, in Fig. 3a. Overall ε increases when U_g increases. However, a considerable dispersion is observed, mainly related to H. Fig. 3a clearly shows that ε is higher in shorter reactors compared to the taller reactors for identical U_g. Different authors (Thorat et al., 1998, Yamashita, 1985, Dhotre, et al., 2004) concluded that the influence of initial liquid height over gas holdup is negligible for H/D over 5 provided that $D \geq 0.15$ m. Nonetheless, the results of the present work clearly show that gas holdup depends on liquid height even at H/D over 40. However, it must be kept in mind that in this work very low superficial gas velocities (one order of magnitude below standard values used in literature (see Dhotre et al., 2004)) have been used in a column with a very small D (0.044 m). As noted above, in this system, the bubbles rise without interacting with each other, there is no coalescence, and d_b is mainly determined by Q, with values between 4.5 and 7 mm for the lower (0.0014 m/s) and higher (0.0057 m/s) gas flow rates,

respectively. These results suggest that instead of using a homographic function of gas velocity, a single dimensionless number including column dimensions (*D* and *H*) would be more appropriate to correlate holdup data.

In this sense, different authors (Akita and Yoshida, 1973; Şal et al., 2013, Shah et al., 2012; Sasaki et al., 2016) have proposed the use of dimensionless numbers such as Reynolds, Archimedes, Galileo, Bond, Weber or Froude to develop general correlations that show the effect of geometric parameters and operation on gas holdup in sparged reactors.

Specifically, the Froude number, *Fr*, which can be derived by scaling of the equation of motion (see Riley et al., 1981), and defined in fluid flow as the ratio of the inertial forces to the gravitational forces, has been proved to be very convenient to represent the effect of mixing in bubble column behaviour (Sanchez-Mirón et al., 2004; Şal et al., 2013). It can be applied to both the bubble and the column (Ruzicka et al., 2008) and has been used traditionally to predict gas holdup in bubble columns (Chisti and Moo Young, 1988; Sasaki et al., 2016). *Fr* can be defined as:

$$Fr = \frac{U}{\sqrt{gL}} \qquad [1]$$

where *U* an *L* are characteristic velocity and length. In the present work the relevant variables were gas flow rate and initial liquid height; thus, using superficial gas velocity, U_g, which includes column diameter, *D*, as characteristic velocity and initial liquid height, *H*, as characteristic length, a global Froude number for the whole bubble column can be written as:

$$Fr_{whole} = \frac{U_g}{\sqrt{gH}} \qquad [2]$$

This Froude number for the gas represents the gas momentum to the gravitational force ratio. Since equation [2] does not justify the effect of d_b in ε, the ratio D/d_b can be included to formulate the following correlation:

$$\varepsilon = a\frac{D}{d_b} \times Fr_{whole} \qquad [3]$$

where a is a constant. In Fig. 3b, gas holdup is plotted according to equation [3], whereby the data nearly collapses onto a single line. Hence Fr_{whole} adequately correlates gas holdup for the range of gas flow rates and liquid heights used in this work. Due to the very low values of Fr_{whole}, gas holdup increases linearly with increasing Fr_{whole}, confirming that the system is well within the bubbly flow regime, as discussed previously. However, it is expected that gas holdup will approach to a certain asymptote as Fr_{whole} increases and the heterogeneous regime is reached. In Fig 3b, CFD predictions for ε have been included.

The overall volumetric mass transfer coefficient, k_La, showed similar behavior to gas holdup (Fig. 4a). In general, k_La increases with U_g. However, k_La decreased with liquid height, as was observed with gas holdup and as previously reported by other authors (Zlokarnik, 1978). The reason is that k_La in the plume is much higher than in the surrounding liquid and the volume ratio from the plume to the surrounding section decreases when liquid height increases. In Fig. 4b k_La is plotted using an equation similar to the equation used for gas holdup:

$$k_La = b\frac{D}{d_b} \times Fr_{whole} \qquad [4]$$

where b is a constant.

Previously, López-Rosales et al. (2017) showed that k_La in this system was not significantly affected by the extension of fluid dynamic forces in the bulk liquid, since

the small changes observed in d_b (between 4.5 and 7 mm) did not produce relevant effects in mass-transfer coefficient (k_L). On the other hand, the similitude between gas holdup and k_La behavior seen in Fig. 3a and 4a, clearly corroborates that k_La rises in a similar fashion as ε. This strongly suggests that the increase in k_La is controlled by gas holdup, which determines interfacial area, and is well established for uniform bubbly flow regimes in gas-driven systems (Contreras et al., 1998; Fernandes et al., 2014).

These results are of critical significance for photobioreactors performance because higher gas flow rates will improve mixing, light reception by the cells and mass transfer, and increase k_La, which in turn will influence the cell growth rate and cell density. However, as noted previously, it is well known that the presence of bubbles may be detrimental for cell viability. Bubble formation at the sparger, bubble rising, and bubble rupture in the interphase can produce relevant cell stress.

Microalgae cell damage in bubble column photobioreactors due to gas sparging is well documented (Barbosa et al., 2003, Sánchez Mirón et al., 2003; Suzuki et al., 1995), although damage was usually quantified indirectly by using liquid flow rate or the superficial gas velocity to correlate experimental results. One of the first steps towards quantification was done by Contreras et al. (1998). They used shear rate and the length of isotropic turbulence micro-eddies, calculated from energy dissipation, to correlate growth rate of *Phaeodactylum tricornutum* in an airlift photobioreactor. Nonetheless, in gas-driven photobioreactors, rational delimitation of harmful events associated with bubbles could help in the optimization of the design and operation of the systems. In this sense, a model has been recently proposed (López-Rosales et al., 2017) to quantify the influence of the presence of bubbles in the growth of the dinoflagellate microalga *K. veneficum*. The model considers the effect of cell damage caused by the presence of

bubbles together with the mass transfer to sustain optimal microalga cell growth. The specific growth rate is described by the equation:

$$\mu = \frac{1}{C_T}\left(\frac{dC_T}{dt}\right) = \frac{\mu_{max}[CO_2]^*\left(1-exp(-k_L a \cdot t)\right)}{K_{CO_2}+[CO_2]^*\left(1-exp(-k_L a \cdot t)\right)} - K_i + K_R' \qquad [5]$$

where μ is the specific growth rate, C_T is the total cell number, $[CO_2]^*$ is the solubility of CO_2, K_{CO2} is the saturation constant, K_i is the specific cell damage-rate constant and K_R' is a specific repair-rate constant. It is well established that cell death does not take place due to bubble rising (Jöbses et al., 1991), therefore the model considers that the events that can potentially damage the cell are the bubble formation at the sparger and the bubble break-up at the culture surface. A specific cell damage rate constant including sub-lethal and lethal damage, derived according to Jöbses et al. (1991) was used:

$$K_i = -k_1 \frac{Q^2 f(d_b)}{V d_b^3 d_0^2 n_0} - k_2 \frac{Q f(d_b)}{V d_b^3} \qquad [6]$$

where k_1 and k_2 are constants, Q is the gas flow rate, V is the volume of the culture, d_0 is the diameter of the sparger nozzle, and n is the number of nozzles. The rate constant defined by equation [6] is proportional to the number of gas bubbles generated per unit time in the sparger (Tramper et al., 1988):

$$K_i \propto \frac{6Q}{\pi d_b^3} \qquad [7]$$

and is just a function of operation variables (Q) and system design parameters (V, d_0, and n). Since the bubble size influences the chance and force of collision between cells and bubbles, according to Jobses et al. (1991) an undefined function of d_b is also included in the rate constant.

The first part of the right side of equation [6] represents the damage associated to the bubble formation at the sparger site and the second part of the right side represents the damage associated to the bubble rupture at the interphase. Since cell damage in each region of the reactor must be associated with energy dissipation, in order to discriminate the relevance of these events, CFD was used to calculate specific energy dissipation in different regions of the bubble column. As mentioned previously, since the Eulerian model does not simulate individual bubbles, the values obtained from the CFD simulations correspond to macroscopic gradients of liquid velocity, not to the energy involved in the individual bubble generation or bursting. Nevertheless, *K. veneficum* cells are robust and their shear-sensitivity comes from the repeated passing of cells through zones of high energy dissipation (Gallardo-Rodríguez et al., 2016), and for that calculation the multiphase model selected is suitable.

In Fig. 5a energy dissipated in the sparger region (ED_{spar}) has been plotted as a function of the *Fr* for the sparger, defined as:

$$Fr_{spar} = \frac{U_{gs}}{\sqrt{g d_0}} \qquad [8]$$

where U_{gs} is the superficial gas velocity in the sparger orifice. Clearly, a linear relationship exists between ED_{spar} and Fr_{spar}.

Similarly, the energy dissipated close to the top region (ED_{top}) has been plotted in Fig. 5b as a function of *Fr* for the top section, defined according to the equation:

$$Fr_{top} = \frac{U_g}{\sqrt{gD}} \qquad [9]$$

To account for different geometrical configuration and operation conditions, and the strong influence of d_b in the energy dissipated in the top, a power function of the ratio D/d_b is also included in the correlation. A linear relationship is also obtained.

In Fig. 5c the average energy dissipated in the column, ED_{whole}, has been plotted with Fr_{whole} defined by equation [2]. A linear relationship is also obtained.

Fig. 5 and equation [8] and [9] elucidate that a relationship exists between energy dissipated in the different zones of the bubble column. The following relationship can be written for energy dissipated in the sparger region and the energy dissipated in the top section of the column:

$$ED_{top} = K_1 \left(\frac{D}{d_b}\right)^4 \left(\frac{d_0}{D}\right)^{5/2} ED_{spar} \qquad [10]$$

Similarly, for ED_{whole} and ED_{spar}:

$$ED_{whole} = K_2 \left(\frac{d_0^5}{D^4 H}\right) ED_{spar} \qquad [11]$$

Equations [10-11] reflect that only D, H, d_0, and d_b determine these relationships.

Since energy dissipation and mass transfer in the bubble column photobioreactor can be described as a function of Froude number, both ED and Fr could be used to represent the influence of hydrodynamics on cell growth in this system. Nonetheless, as shown in Fig. 6a-c, the growth of *K. veneficum* only correlates with ED_{whole} (not with ED_{spar} or ED_{top}). Fig. 6c shows the specific growth rate and biomass productivity after 5 days of *K veneficum* as a function of ED_{whole}/H. This figure shows that for low energy dissipation, cell growth and productivity increase when ED_{whole}/H increases, reaching a maximum followed by a marked decrease in both parameters. This pattern strongly point out the existence of mass transfer limitations at low energy dissipation and cell

stress above a defined value of ED_{whole}/H. In this figure, the data for the outdoor pilot-scale bubble column and flat panel have been included (López-Rosales et al., 2018).

Although the molecular basis of the mechanism by which fluid forces are converted into a cellular signal in dinoflagellate microalgae remains unknown, their sensitivity to hydrodynamic forces has been clearly shown to be similar to that for animal cells (López-Rosales et al; 2015). Irrespective of the mechanism, the result is that excessive hydrodynamic forces drive regulation of gene expression, thus producing critical changes in cell physiology (Los et al., 2013). These changes include the overproduction of ROS, generating oxidative stresses that lead to the rigidification of the cell and thylakoid membranes. It is well established that cell membrane acts as a flow sensor with transducers that trigger different metabolic responses (Chen et al., 2007), including bioluminescence, and has been proven that inhibitory levels of shear stress leads to a decrease in membrane fluidity (Gallardo-Rodriguez et al., 2012), which may provide a preventative capacity against predator grazing (López-Rosales et al., 2015). Otherwise, rigidification of thylakoid membranes undoubtedly affects photosynthetic machinery, especially to its most vulnerable component, photosystem II, suppressing the de novo synthesis of the D1 protein, a critical piece of its photochemical reaction centre (Nishiyama et al., 2004).

To corroborate if the model represented by equation [5] can be used to describe the influence of energy dissipation on the growth of *K. veneficum*, a specific cell damage-rate constant has been defined as:

$$K_i = -k_3 \left(\frac{ED_{whole}}{H}\right)^c \qquad [12]$$

where k_3 and c are constants with values of 10 and 0.96. As shown in Fig. 6d, the model adequately describes the influence of ED_{whole}/H in the growth of *K. veneficum*. Equation

[5] with K_i given by equation [12] correlates more than 80% of the data with less than 20% error. The model also represents satisfactorily data of a pilot scale bubble column and flat panel (López-Rosales et al., 2018). It is evident from Fig. 6 that this model provided insight into the relevance of dissipated energy in the overall performance of photobioreactors for shear-sensitive microalgae culture, irrespective of size and geometry and has to be carefully considered for an optimal design and industrial operation.

4. Conclusions

In this study, CFD was used to simulate hydrodynamics in a bubble column photobioreactor. Distribution of gas holdup, liquid velocity and specific energy dissipation rate were obtained for different culture height, gas velocities and nozzle diameter. Gas holdup, energy dissipation and mass transfer correlated well with Froude number. This work presents the first study to substantiate that *K. veneficum* growth was limited by CO_2 transfer depending on the threshold of energy dissipation and a fluid dynamic stress. Complementary CFD predictions were used to explain the experimental observations and develop correlations that can be used for other similar homogenous flows.

Acknowledgements

This research was funded by the Spanish Ministry of Economy and Competitiveness (grant CTQ2014-55888-C3-02) and the European Regional Development Fund Program.

References

1. Akita, K., Yoshida, F., 1973. Gas holdup and volumetric mass transfer coefficient in bubble columns. Effects of liquid properties. Ind. Eng. Chem. Process. Des. Dev. 12(1), 76-80.
2. Barbosa, M. J., Albrecht, M., Wijffels, R. H., 2003. Hydrodynamic stress and lethal events in sparged microalgae cultures. Biotechnol. Bioeng. 83(1), 112-120.
3. Bitog, J. P. P., Lee, I. B., Oh, H. M., Hong, S. W., Seo, I. H., Kwon, K. S., 2014. Optimised hydrodynamic parameters for the design of photobioreactors using computational fluid dynamics and experimental validation. Biosyst. Eng. 122, 42-61.
4. Carvalho, A. P., Meireles, L. A., Malcata, F. X., 2006. Microalgal reactors: a review of enclosed system designs and performances. Biotechnol. Prog. 22(6), 1490-1506.
5. Chen, A. K., Latz, M. I., Sobolewski, P., Frangos, J. A., 2007. Evidence for the role of G-proteins in flow stimulation of dinoflagellate bioluminescence. Am. J. Physiol. Regul. Integr. Comp. Physiol. 292(5), R2020-R2027.
6. Chisti, M. Y., Moo-Young, M., 1988. Hydrodynamics and oxygen transfer in pneumatic bioreactor devices. Biotechnol. Bioeng. 31(5), 487-494.
7. Contreras, A., García, F., Molina, E., Merchuk, J. C., 1998. Interaction between CO_2-mass transfer, light availability, and hydrodynamic stress in the growth of *Phaeodactylum tricornutum* in a concentric tube airlift photobioreactor. Biotechnol. Bioeng. 60(3), 317-325.
8. Dhotre, M. T., Ekambara, K., Joshi, J. B., 2004. CFD simulation of sparger design and height to diameter ratio on gas hold-up profiles in bubble column

reactors. Exp. Therm. Fluid Sci. 28, 407-421.Duchemin, L., Popinet, S., Josserand, C., Zaleski, S., 2002. Jet formation in bubbles bursting at a free surface. Phys. Fluids. 14 (9): 3000-3008.

9. Duchemin, L., Popinet, S., Josserand, C., Zaleski, S., 2002. Jet formation in bubbles bursting at a free surface. Phys. Fluids. 14(9): 3000-3008.
10. Fernandes, B. D., Mota, A., Ferreira, A., Dragone, G., Teixeira, J. A., Vicente, A. A., 2014. Characterization of split cylinder airlift photobioreactors for efficient microalgae cultivation. Chem. Eng. Sci. 117, 445-454.
11. Ferreira, A., Cardoso, P., Teixeira, J. A., Rocha, F., 2013. pH influence on oxygen mass transfer coefficient in a bubble column. Individual characterization of k_L and a. Chem. Eng. Sci. 100, 145-152.
12. Ferreira, B. S., Fernandes, H. L., Reis, A., Mateus, M., 1998. Microporous hollow fibres for carbon dioxide absorption: mass transfer model fitting and the supplying of carbon dioxide to microalgal cultures. J. Chem. Technol. Biotechnol. 71(1), 61-70.
13. Gallardo-Rodríguez, J. J., García-Camacho, F., Sánchez-Mirón, A., López-Rosales, L., Chisti, Y., Molina-Grima, E., 2012. Shear-induced changes in membrane fluidity during culture of a fragile dinoflagellate microalga. Biotechnol. Prog. 28(2), 467-473.
14. Gallardo-Rodríguez, J.J., López-Rosales, L., Sánchez-Mirón, A., García-Camacho, F., Molina-Grima, E., Chalmers, J.J., 2016. New insights into shear-sensitivity in dinoflagellate microalgae. Bioresour. Technol. 200, 699–705.
15. García-Camacho, F., Contreras-Gómez, A., Mazzuca-Sobczuk, T., Molina-Grima, E., 2000. Effects of mechanical and hydrodynamic stress in agitated,

sparged cultures of *Porphyridium cruentum*. Process Biochem. 35(9), 1045-1050.

16. Gudin, C., Chaumont, D., 1991. Cell fragility—the key problem of microalgae mass production in closed photobioreactors. Bioresour. Technol. 38(2-3), 145-151.
17. Guillard, R. R. L., Hargraves, P. E., 1993. *Stichochrysis immobilis* is a diatom, not a chrysophyte. Phycologia 32(3), 234-236.
18. Hu, W., Berdugo, C., Chalmers, J. J., 2011. The potential of hydrodynamic damage to animal cells of industrial relevance: current understanding. Cytotechnology 63(5), 445.
19. Jöbses, I., Martens, D., Tramper, J., 1991. Lethal events during gas sparging in animal cell culture. Biotechnol. Bioeng. 37(5), 484-490.
20. Liu, Y., Li, F., Hu, W., Wiltberger, K., Ryll, T., 2014. Effects of bubble–liquid two-phase turbulent hydrodynamics on cell damage in sparged bioreactor. Biotechnol. Prog. 30(1), 48-58.
21. López-Rosales, L., García-Camacho, F., Sánchez-Mirón, A., Contreras-Gómez, A., Molina-Grima, E., 2015. An optimisation approach for culturing shear-sensitive dinoflagellate microalgae in bench-scale bubble column photobioreactors. Bioresour. Technol. 197, 375-382.
22. López-Rosales, L., García-Camacho, F., Sánchez-Mirón, A., Contreras-Gómez, A., Molina-Grima, E., 2017. Modeling shear-sensitive dinoflagellate microalgae growth in bubble column photobioreactors. Bioresour. Technol. 245, 250-257.
23. López-Rosales, L., Sánchez-Mirón, A., García-Camacho, F., Place, A. R., Chisti, Y., Molina-Grima, E., 2018. Pilot-scale outdoor photobioreactor culture

of the marine dinoflagellate Karlodinium veneficum: Production of a karlotoxins-rich extract. Bioresour. Technol. 253, 94–104

24. Los, D. A., Mironov, K. S., Allakhverdiev, S. I., 2013. Regulatory role of membrane fluidity in gene expression and physiological functions. Photosyn. Res. 116(2-3), 489-509.
25. Manjrekar, O. N., Sun, Y., He, L., Tang, Y. J., Dudukovic, M. P., 2017. Hydrodynamics and mass transfer coefficients in a bubble column photo-bioreactor. Chem. Eng. Sci. 168, 55-66.
26. Meier, S. J., Hatton, T. A., Wang, D. I., 1999. Cell death from bursting bubbles: role of cell attachment to rising bubbles in sparged reactors. Biotechnol. Bioeng. 62(4), 468-478.
27. Molina-Grima, E., Sánchez-Pérez, J., García-Camacho, F., Robles-Medina, A., 1993. Gas-liquid transfer of atmospheric CO_2 in microalgal cultures. J. Chem. Technol. Biotechnol. 56(4), 329-337.
28. Mollet, M., Ma N., Zhao, Y., Brodkey, R., Taticek, R., Chalmers, J. J., 2004. Bioprocess equipment: Characterization of energy dissipation rate and its potential to damage cells. Biotechnol. Prog. 20, 1437-1448.
29. Nedeltchev, S., Nigam, K. D., Schumpe, A., 2014. Prediction of mass transfer coefficients in a slurry bubble column based on the geometrical characteristics of bubbles. Chem. Eng. Sci. 106, 119-125.
30. Nishiyama, Y., Allakhverdiev, S. I., Yamamoto, H., Hayashi, H., Murata, N., 2004. Singlet oxygen inhibits the repair of photosystem II by suppressing the translation elongation of the D1 protein in *Synechocystis* sp. PCC 6803. Biochemistry 43(35), 11321-11330.

31. Pegallapati, A. K., Nirmalakhandan, N., 2012. Modeling algal growth in bubble columns under sparging with CO_2-enriched air. Bioresour. Technol. 124, 137-145.

32. Pfleger, D., Becker, S., 2001. Modelling and simulation of the dynamic flow behaviour in a bubble column. Chem. Eng. Sci. 56(4), 1737-1747.

33. Riley, J. J., Metcalfe, R. W., Weissman, M. A., 1981. Direct numerical simulations of homogeneous turbulence in density-stratified fluids, in West, B. J. (Ed.), Proc. of the AIP Conference on Nonlinear Properties of Internal Waves. American Institute of Physics, New York, pp. 79-112.

34. Ruzicka, M. C., Vecer, M. M., Orvalho, S., Drahoš, J., 2008. Effect of surfactant on homogeneous regime stability in bubble column. Chem. Eng. Sci. 63(4), 951-967.

35. Şal, S., Gül, Ö. F., Özdemir, M., 2013. The effect of sparger geometry on gas holdup and regime transition points in a bubble column equipped with perforated plate spargers. Chem. Eng. Process.: Process Intensif. 70, 259-266.

36. Sánchez-Mirón, A., Cerón-García, M. C, Contreras-Gómez, A., García-Camacho, F., Molina-Grima, E., Chisti, Y., 2003. Shear stress tolerance and biochemical characterization of *Phaeodactylum tricornutum* in quasi steady-state continuous culture in outdoor photobioreactors. Biochem. Eng. J. 16(3), 287-297.

37. Sánchez-Mirón, A., Cerón-García, M. C., García-Camacho, F., Molina-Grima, E., Chisti, Y., 2004. Mixing in bubble column and airlift reactors. Chem. Eng. Res. Des. 82(10), 1367-1374.

38. Sánchez-Mirón, A., García-Camacho, F., Contreras-Gómez, A., Molina-Grima, E., Chisti, Y., 2000. Bubble-column and airlift photobioreactors for algal culture. AIChE J. 46(9), 1872-1887.

39. Sasaki, S., Hayashi, K., Tomiyama, A., 2016. Effects of liquid height on gas holdup in air–water bubble column. Exp. Therm. Fluid Sci. 72, 67-74.

40. Shah, M., Kiss, A. A., Zondervan, E., van der Schaaf, J., de Haan, A. B., 2012. Gas holdup, axial dispersion, and mass transfer studies in bubble columns. Ind. Eng. Chem. Res. 51(43), 14268-14278.

41. Silva, H. J., Cortifas, T., Ertola, R. J., 1987. Effect of hydrodynamic stress on *Dunaliella* growth. J. Chem. Technol. Biotechnol. 40(1), 41-49.

42. Suzuki, T., Matsuo, T., Ohtaguchi, K., Koide, K., 1995. Gas-sparged bioreactors for CO_2 fixation by *Dunaliella tertiolecta*. J. Chem. Technol. Biotechnol. 62(4), 351-358.

43. Thorat, B. N., Shevade, A. V., Bhilegaonkar, K. N., Aglawe, R. H., Veera, U. P., Thakre, S. S., Pandit, A. B., Joshi, J. B., 1998. Effect of sparger design and height to diameter ratio on fractional gas hold-up in bubble columns. Trans. IChemE. 76(Part A).

44. Tramper, J., Smit, D., Straatman, J., Vlak, J. M., 1988. Bubble-column design for growth of fragile insect cells. Bioprocess Eng. 3(1), 37-41.

45. Wu, Y., Ong, B. C., Al-Dahhan, M. H., 2001. Predictions of radial gas holdup profiles in bubble column reactors. Chem. Eng. Sci. 56(3), 1207-1210.

46. Yamashita, F., 1985. Effect of liquid depth, column inclination and baffle plates on gas holdup in bubble columns. J. Chem. Eng. Jpn. 18(4), 349-353.

47. Zhao, L., Li, J., Battaglia, F., He, Z., 2016a. Investigation of multiphysics in tubular microbial fuel cells by coupled computational fluid dynamics with multi-

order Butler-Volmer reactions. Chem. Eng. J. 296(7), 377–385.

48. Zhao, L., Li, J., Battaglia, F., He, Z., 2016b. Computational investigation of the flow field contribution to improve electricity generation in granular activated carbon-assisted microbial fuel cells. J. Power Sources 333(11), 83-87.

49. Zhu, Y., Cuenca, J. V., Zhou, W., Varma, A., 2008. NS0 cell damage by high gas velocity sparging in protein-free and cholesterol-free cultures. Biotechnol. Bioeng. 101(4), 751-760.

50. Zlokarnik, M., 1978. Sorption characteristics for gas-liquid contacting in mixing vessels. Advan. Biochem. Eng. 8, 133-151.

Figure legends

Fig.1. Gas holdup (a), water velocity vectors (b), and local energy dissipation rate (c) averaged over 30 s in a longitudinal x-y plane, and radial profiles of gas holdup (d), water velocity (e) and energy dissipation rate (f) for the shorter column (H = 0.5 m, U_g = 0.0028 m s^{-1}, d_0 = 1.5 mm) at different locations of that plane.

Fig. 2. Gas holdup (a), water velocity vectors (b), and local energy dissipation rate (c) averaged over 30 s in a longitudinal x-y plane, and radial of gas holdup (d), water velocity (e) and energy dissipation rate (f) for the higher column (H = 1.75 m, U_g = 0.0014 m s^{-1}, d_0 = 2 mm) at different locations of that plane.

Fig. 3. Influence of superficial gas velocity on the experimental gas holdup (a) and correlation of ε with Fr_{whole} number (b). Numbers in (a) indicate the culture height in each experiment. All data points represent mean values from experiments performed in duplicate. Gas holdup values simulated with CFD have been included in Fig. 3b.

Fig. 4. Influence of superficial gas velocity on the overall mass transfer coefficient (a) and correlation of k_La with Fr_{whole} number (b). Numbers in (a) indicate the culture height in each experiment. All data points represent mean values from experiments performed in duplicate.

Fig. 5. Correlation of energy dissipated in the sparger zone, ED_{spar} (a), near the head space, ED_{top} (b) and whole column, ED_{whole} (c) obtained with computational fluid dynamics, with Fr number defined for each zone.

Fig. 6. Influence of ED_{spar} (a), ED_{top} (b), and ED_{whole} (c) on the maximum growth rate (μ) and biomass productivity after 5 days (P_b) and comparison of the experimental growth rate and values calculates according to equation [5] (d). The diagonal represent

an exact agreement. Data for outdoor pilot bubble column and flat panel have been included.

Figure 1

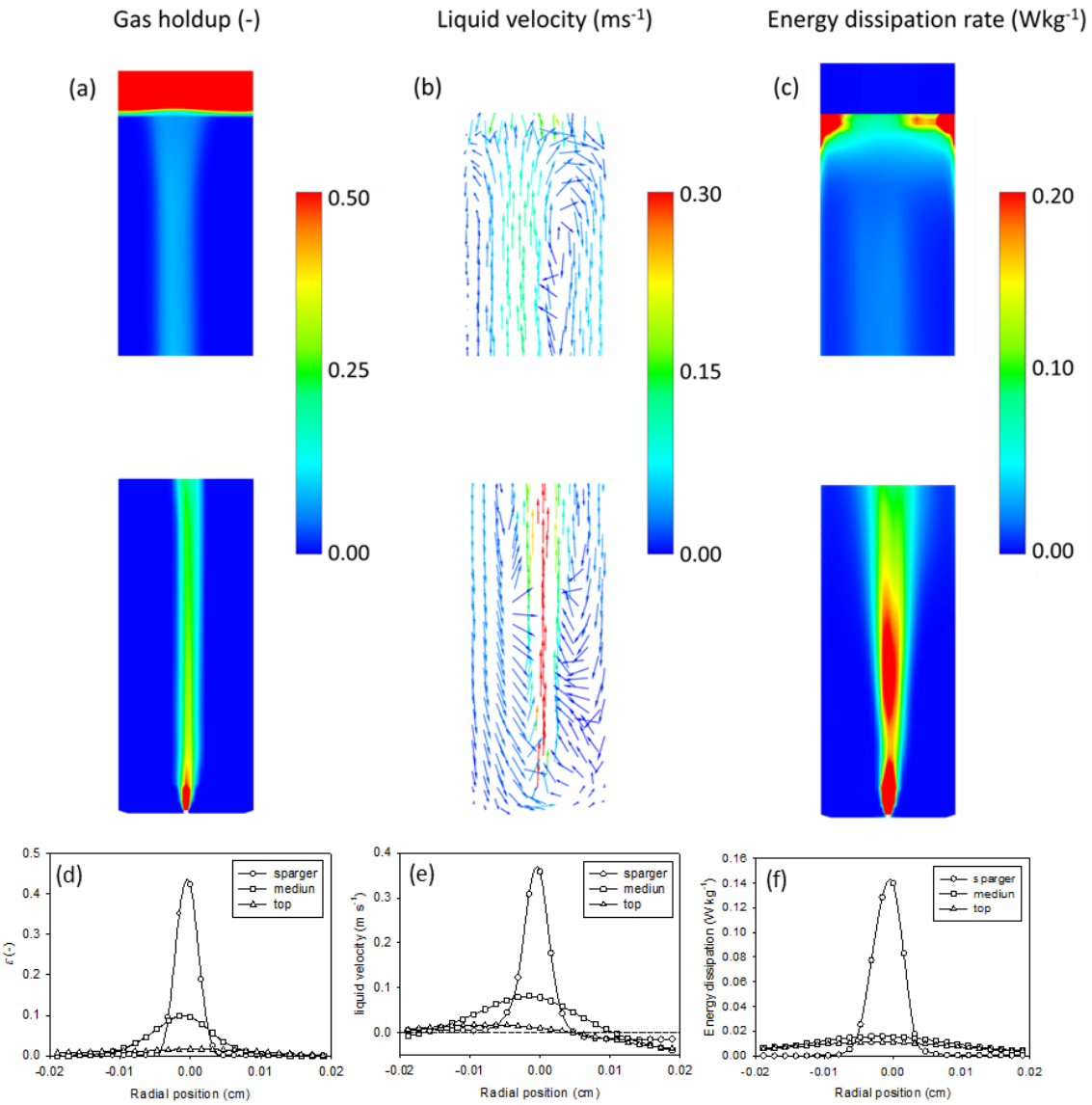

Figure2

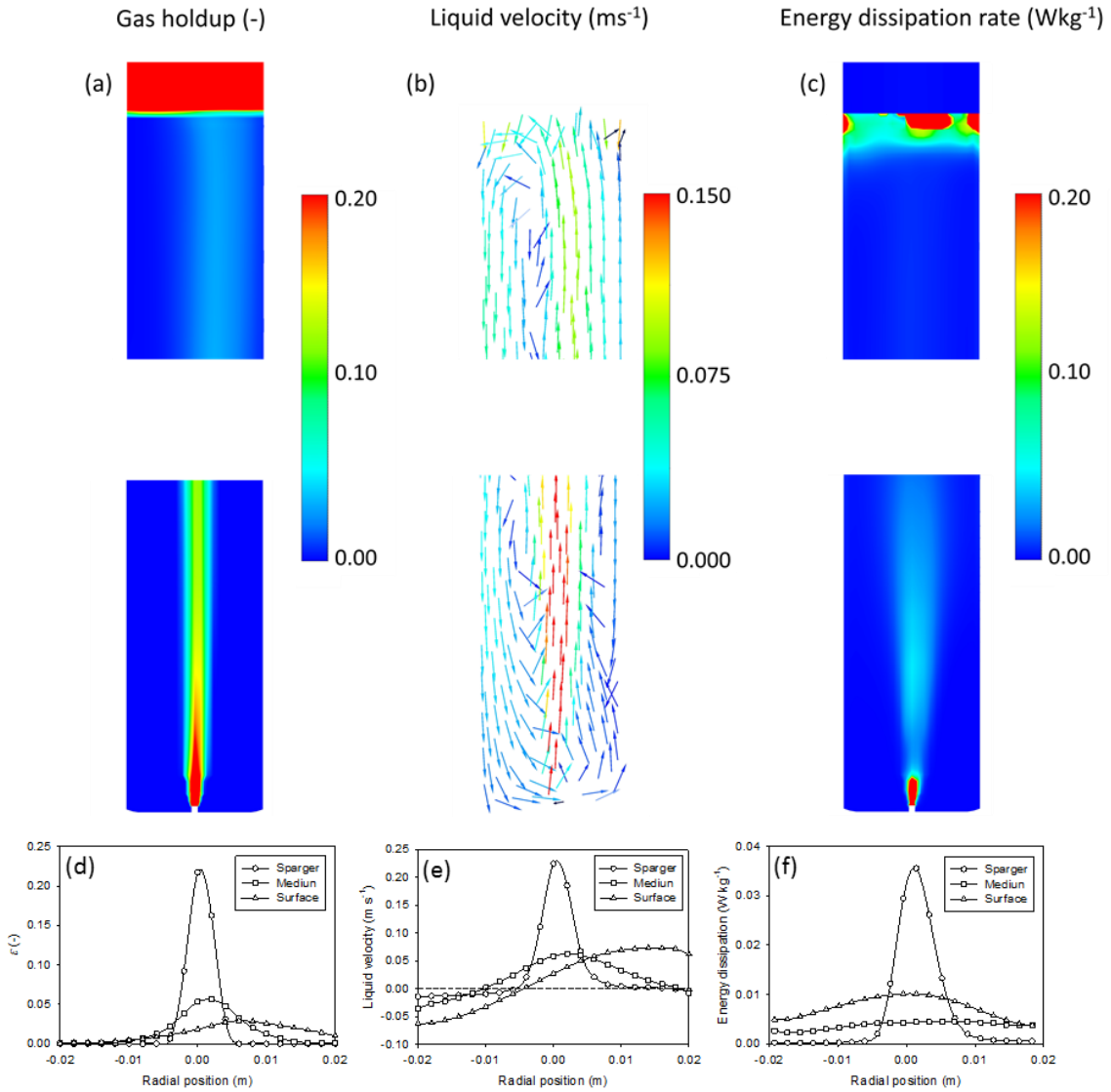

Figure 3

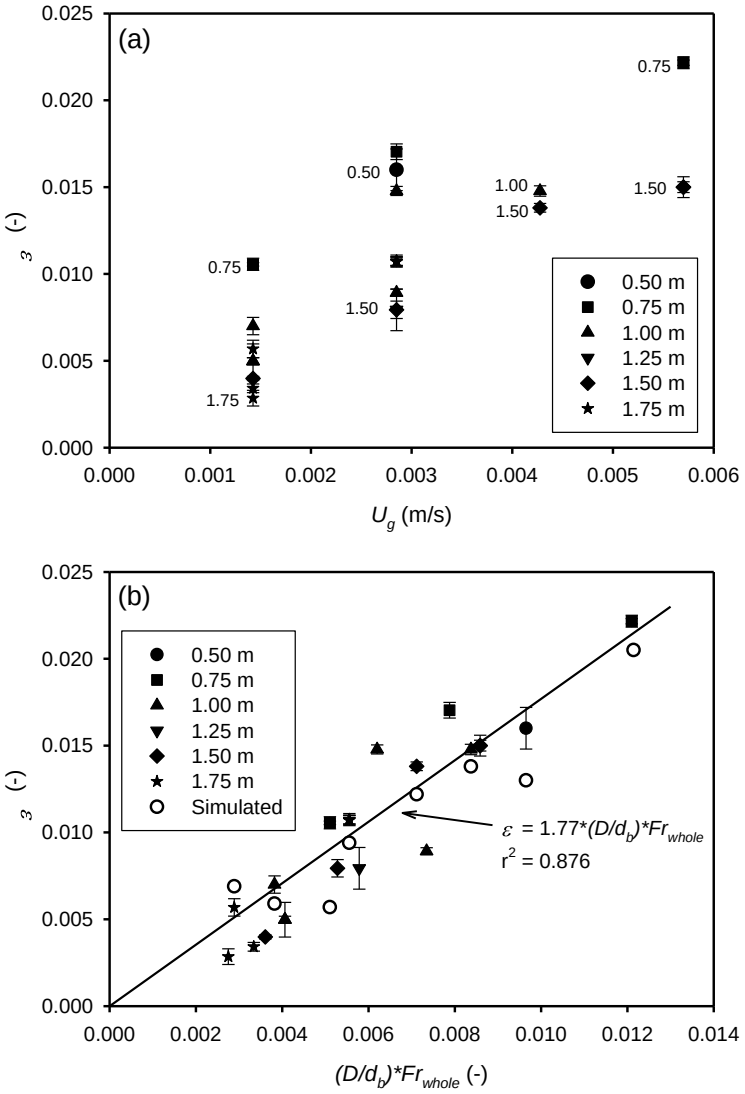

Figure 4

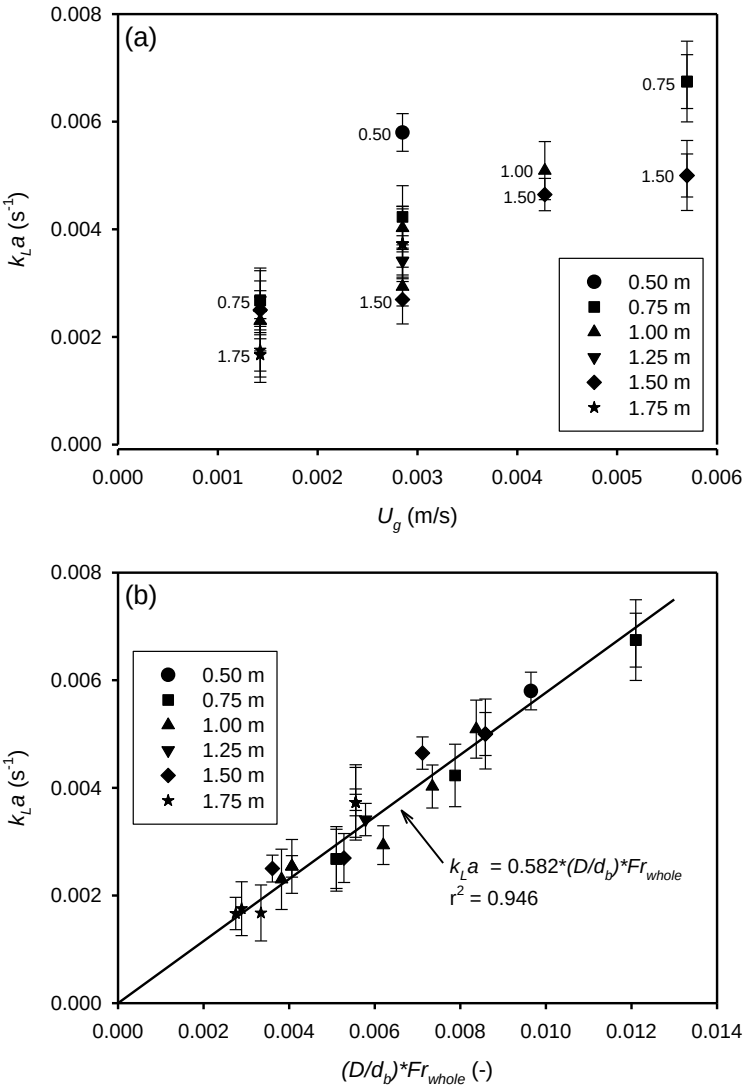

Figure 5

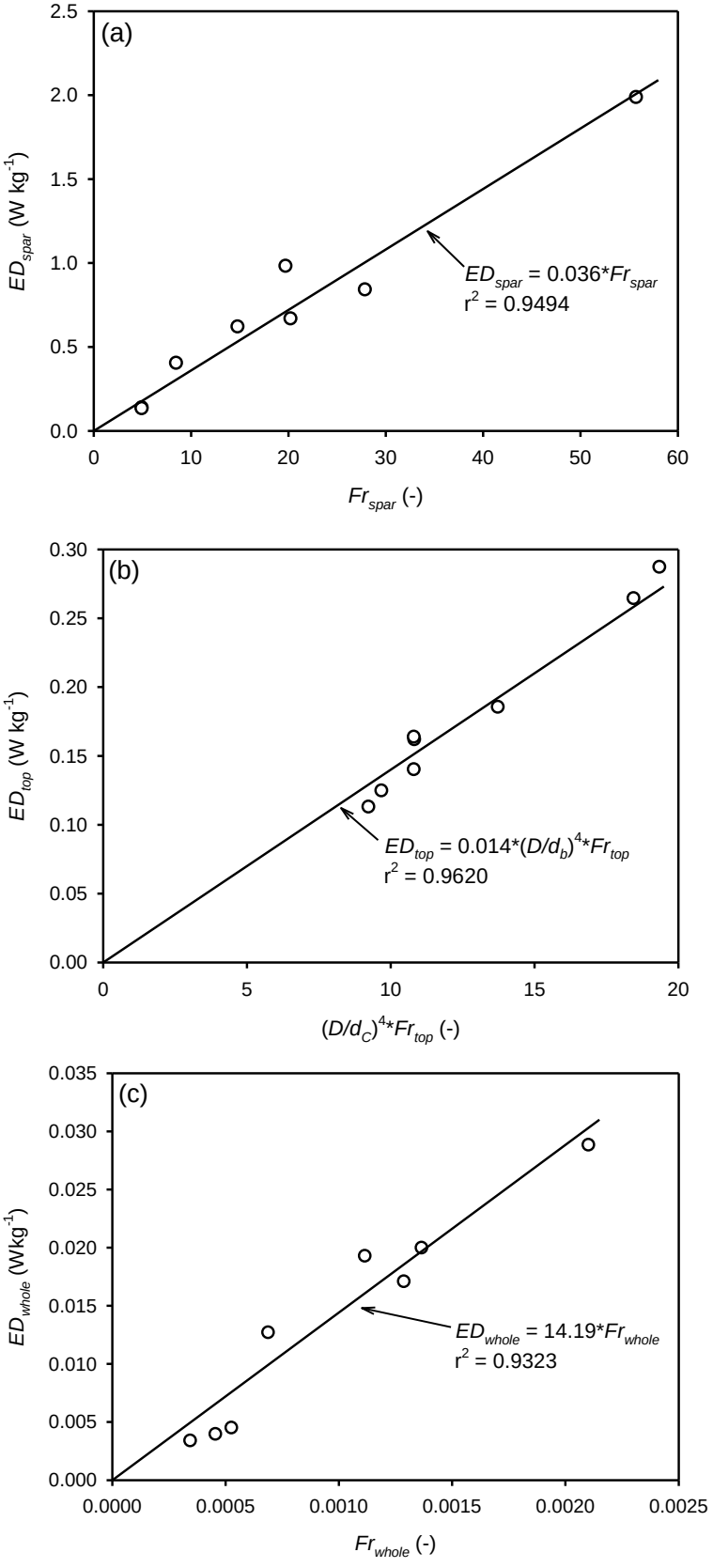

Figure 6